

Lanthanide Organic Framework as a Regenerable Luminescent Probe for Fe<sup>3+</sup>

Hang Xu, Huan-Cheng Hu, Chun-Shuai Cao, and Bin Zhao\*

Department of Chemistry, Key Laboratory of Advanced Energy Material Chemistry, MOE, and Collaborative Innovation Center of Chemical Science and Engineering (Tianjin), Nankai University, Tianjin 300071, China

## Supporting Information

**ABSTRACT:** A unique three-dimensional Tb-BTB framework (**1**) with two types of one-dimensional channels was obtained and structurally characterized, exhibiting high thermal stability. Luminescent investigations reveal that **1** can detect Fe<sup>3+</sup> with relatively high sensitivity and selectivity. Importantly, **1** as the luminescent probe of Fe<sup>3+</sup> can be simply and quickly regenerated, which represents a rare example in reported luminescent sensors of Fe<sup>3+</sup>.

Lanthanide-based metal–organic frameworks (Ln-MOFs) have been receiving considerable attention because of their diversified structures,<sup>1–7</sup> intriguing magnetism,<sup>8</sup> and optical properties.<sup>2–6,9,10</sup> Ln-MOFs with high porosity can be considered as highly sensitive and selective luminescent sensors because some small molecules/ions can diffuse in and get out of channels quickly, and these MOFs have the potential for recycling. In the past decade, quite a lot of effort has been made on Ln-MOFs for the detection of Cu<sup>2+</sup>, Zn<sup>2+</sup>, Mg<sup>2+</sup>, F<sup>−</sup>, nitrobenzene, dinitrotoluene, and so on.<sup>10,4,11–14</sup> However, only a few examples were associated with the luminescent probe for Fe<sup>3+</sup> ions,<sup>4,11–14</sup> which play an important role in biological systems and have wide applications in industry production.<sup>4,14</sup> In these studies, the selectivity and sensitivity to Fe<sup>3+</sup> were mainly investigated, but few investigations on the recyclable performance of Fe<sup>3+</sup> sensors were carried out.

In this contribution, we selected benzene-1,3,5-tribenzoate (H<sub>3</sub>BTB) as a classical ligand to construct Ln-MOFs based on the following considerations: (1) high C<sub>3</sub> symmetry and large molecule size are a benefit to forming the highly porous and robust frameworks; (2) the high-performance antenna effect originating from the largely electronic conjugate system in H<sub>3</sub>BTB can make energy easily transferable to lanthanide luminescent centers. Up to now, most of the MOFs based on the H<sub>3</sub>BTB ligand focused on transition metals, such as MOF-14,<sup>15a</sup> MOF-177,<sup>15b</sup> DUT-9,<sup>15c</sup> etc.<sup>16</sup> However, to the best of our knowledge, only two Ln-MOFs associated with the H<sub>3</sub>BTB ligand were investigated,<sup>17</sup> in which gas adsorption was mainly studied and the luminescent properties attracted little attention. Herein, a unique three-dimensional (3D) stable framework, {[Tb(BTB)(DMF)]·1.5DMF·2.5H<sub>2</sub>O}<sub>n</sub> (**1**; DMF = *N,N*-dimethylformamide), displaying two types of one-dimensional (1D) channels was successfully obtained. The luminescent explorations revealed that compound **1** belongs to the recyclable

MOF luminescent probe for Fe<sup>3+</sup> ions, possessing relatively high selectivity and sensitivity among 15 kinds of metal ions.

By a solvothermal method, Tb(NO<sub>3</sub>)<sub>3</sub> combined with H<sub>3</sub>BTB in the presence of LiOH produced a 3D framework at about 85% yield. Single-crystal X-ray diffraction shows that compound **1** crystallizes in the *P2*<sub>1</sub>/*c* space group. The asymmetric unit consists of one Tb<sup>3+</sup> ion, one BTB<sup>3−</sup> anion, one coordinated DMF, 1.5 lattice DMF, and 2.5 lattice H<sub>2</sub>O. An eight-coordinated Tb<sup>3+</sup> ion exhibits a distorted square-antiprism geometry,<sup>18</sup> which is completed by seven carboxylic oxygen atoms and one coordinated DMF (Figure 1a). The Tb–O<sub>carboxyl</sub> bond lengths

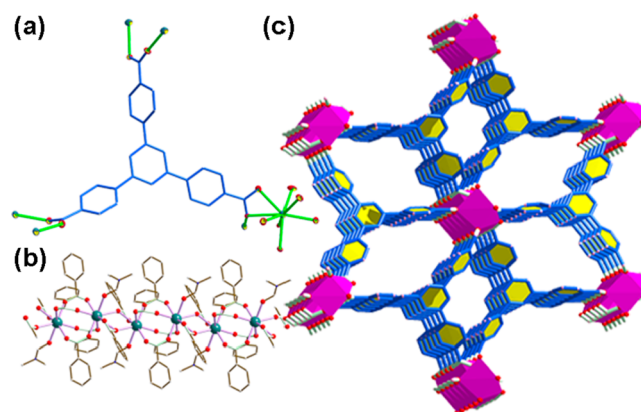


**Figure 1.** (a) Coordinated environment of Tb<sup>3+</sup>. (b) Tb<sup>3+</sup> connected to a 1D chain by carboxyl bridges. (c) 3D framework with two types of 1D channels along the *a* direction.

fall in the reasonable range of 2.310–2.579 Å,<sup>2,19a</sup> and adjacent Tb<sup>3+</sup> ions are bridged by carboxylate groups into the terbium chain with a Tb...Tb distance of 4.103–4.226 Å (Figure 1b). The structural feature of **1** is that each terbium chain serves as a secondary building unit and is further connected by a BTB<sup>3−</sup> ligand into a 3D framework, containing two types of 1D channels with diameters of 4.60 and 3.25 Å along the *a* direction, respectively (Figure 1c). The total potential pore volume of open channels in **1** is about 38.5%, as calculated by the PLATON program. In addition, thermogravimetric analysis (TGA) of **1** (Figure S6 in the Supporting Information, SI) reveals that the weight loss of 18.31%, consistent with the theoretical value (18.79%), is attributed to the loss of coordinated and free solvent

Received: January 20, 2015

Published: May 7, 2015

molecules, and the 3D framework of **1** possesses high thermal stability.<sup>19</sup> To further explore the thermal stability of **1**, the X-ray thermodiffractogram of **1** was measured under air, and the intensity of characteristic peaks gradually decreases as the temperature increases. At 480 °C, **1** begins a transformation from the crystalline to the amorphous state (Figure S7 in the SI). The results indicate that compound **1** has a high thermostability and keeps the crystalline phase at high temperature.

The luminescence spectrum of **1** is shown in Figure S8 in the SI at room temperature. Under excitation at 300 nm, **1** exhibits four characteristic emission peaks at 490, 545, 585, and 622 nm, which are assignable to  $^5D_4 \rightarrow ^7F_J$  ( $J = 6, 5, 4, 3$ ) transitions of the  $Tb^{3+}$  ion, respectively.<sup>20</sup> The strongest  $^5D_4 \rightarrow ^7F_5$  transition, showing green-light emission, is attributed to magnetic-dipole-induced transitions.<sup>20</sup>

To investigate the influence of different metal ions on the luminescence of **1**, 4 mg of **1** was dispersed in 3.6 mL of an ethanol solution, forming a suspension solution by an ultrasound method, and 400  $\mu$ L of an ethanol solution of  $M(NO_3)_x$  ( $1 \times 10^{-2}$  M;  $M = Fe^{3+}, Li^+, Na^+, K^+, Cs^+, Mg^{2+}, Ca^{2+}, Sr^{2+}, Ba^{2+}, Pb^{2+}, Zn^{2+}, Mn^{2+}, Cd^{2+}, Co^{2+}, Ni^{2+}, Fe^{2+}, Cr^{3+}, Cu^{2+}$ , respectively) was slowly dropped into the above solutions to form a suspension of metal-**1** in ethanol ( $1 \times 10^{-3}$  M). The corresponding luminescence curve still shows the four characteristic emission peaks (Figure S9 in the SI) of  $Tb^{3+}$  ions, and only the highest emission peaks at 545 nm were monitored under the perturbation of various cations (Figure 2). Interestingly,  $Fe^{3+}$

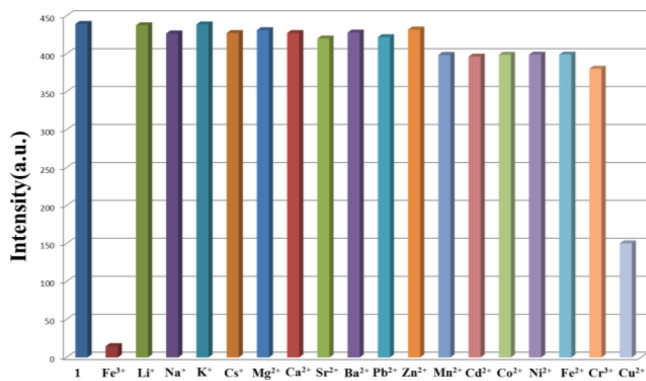


**Figure 2.** Comparison of the luminescence intensity of the  $^5D_4 \rightarrow ^7F_5$  transition (545 nm) of  $M^{n+}$ -**1** in  $10^{-3}$  M different metal ions.

exhibits a drastic quenching effect on the luminescence of **1**, while other metal ions have no significant effect on the emission with the exception of  $Cu^{2+}$ , which can weaken the luminescence to some extent. The different effects on the emission between  $Fe^{3+}$  and other cations are clearly observed, indicative of the fact that **1** can be considered as a promising luminescent probe for  $Fe^{3+}$  ions. Furthermore, to study the influence of mixed cations on the emission of **1**, 0.4 mL of  $Fe^{3+}$  ( $1 \times 10^{-2}$  M) and 0.4 mL of ethanol solutions of other cations ( $1 \times 10^{-2}$  M) were slowly dropped into a 3.2 mL suspension of **1** in ethanol, respectively. The quenching effect of  $Fe^{3+}$  on **1** is not influenced by the introduced metal ions (Figure S10 in the SI), suggesting that **1** can selectively detect  $Fe^{3+}$  ions among the above cations.

Moreover, to explore the detection limit of **1** as a  $Fe^{3+}$  probe,  $Fe^{3+}$  with different concentrations in ethanol solutions were dropped into a suspension of **1** to form a series of suspensions of  $Fe^{3+}$ -**1** in ethanol ( $10^{-5}$ – $10^{-3}$  mol/L). The luminescence intensity of **1** gradually decreases with increasing concentration

of  $Fe^{3+}$ , and the decrease of the luminescence intensity is still clearly observed when **1** is immersed in a  $10^{-5}$  mol/L  $Fe^{3+}$  solution (Figure 3), indicating that the detection limit of **1** as a

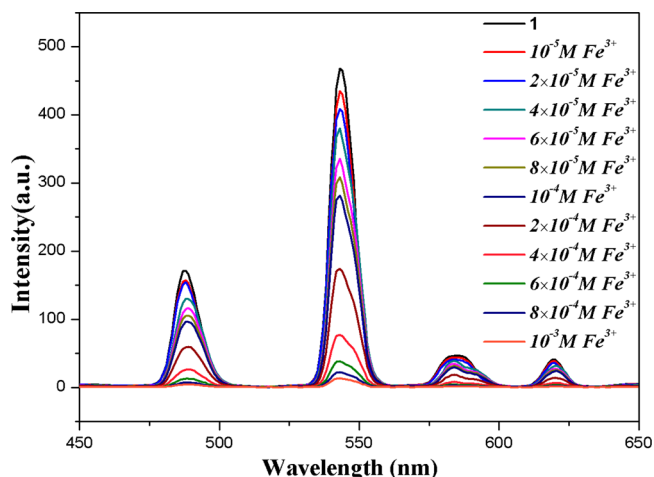


**Figure 3.** Comparison of the luminescence intensity of compound **1** immersed in different concentrations (mol/L) of  $Fe(NO_3)_3$  ethanol solutions.

$Fe^{3+}$  probe can reach  $10^{-5}$  mol/L. As illustrated in Table S2 in the SI, most of the reported MOFs can detect  $Fe^{3+}$  with concentrations from  $10^{-3}$  to  $10^{-5}$  M, and the lowest detected concentration of  $Fe^{3+}$  was recorded in MIL-53(Al). Comparably, **1** exhibits relatively high sensitivity and selectivity. To further study the relationship between the  $Fe^{3+}$  concentration and quenching effect, a plot of the luminescence intensity versus  $Fe^{3+}$  concentration was made (Figure S11 in the SI), which can not be well fitted by the Stern–Volmer equation, indicating the coexistence of the dynamic and static quenching processes.<sup>21</sup>

It should be noted that the recyclable capacity was not explored in reported MOF-based sensors as  $Fe^{3+}$ . Considering the cost of luminescent probes, nonrecyclable probes with low yield are not extensively employed in practical applications. Therefore, the regenerable performance and high yield play important roles in luminescent probes. Luckily, on the basis of  $Tb(NO_3)_3 \cdot 6H_2O$ , the yield of **1** is as high as 85%.

On the other hand, fast and simple regeneration methods are two important topics about the recyclable performance. Herein, to investigate the recyclable performance of **1**, we attempted to immerse **1** in an ethanol solution of  $10^{-3}$  M  $Fe^{3+}$  ions for minutes to form  $Fe^{3+}$ -**1**, and then  $Fe^{3+}$ -**1** was washed with ethanol several times. The luminescence intensity and powder XRD (PXRD) of the recycled **1** are well consistent with the simulated one from **1**, and three runs were performed (Figure 4 and S14 in the SI). The results indicate that the framework of **1** is still stable and **1** can be recycled by a fast and simple method. Furthermore, there is no feature peak of  $Fe^{3+}$  in X-ray photoelectron spectroscopy (XPS; Figure S12 in the SI), indicating that the introduced  $Fe^{3+}$  ions have been removed completely.

In previous studies, MOFs captured  $Fe^{3+}$  ions by cation exchange or a strong interaction between the frameworks and introduced  $Fe^{3+}$  ions.<sup>4,11–14</sup> As for **1**, the discussions were given as follows: (1) PXRD of  $Fe^{3+}$ -**1** (Figure S5 in the SI) was carried out, proving that the 3D framework of **1** still remained intact and the luminescence quenching was not caused by collapse of the framework; (2) it was difficult for the neutral MOFs of **1** to capture  $Fe^{3+}$  by exchanging cation methods; (3) energy-

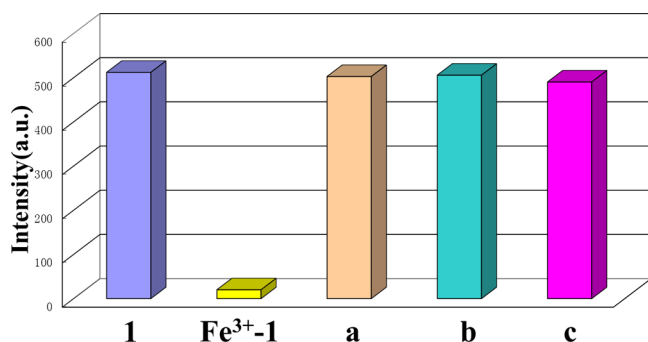


**Figure 4.** The luminescence intensity (545 nm) of three recycles (a) after the first recycle, (b) after the second recycle, and (c) after the third recycle.

dispersive spectrometry investigations of Fe<sup>3+</sup>-1 clearly indicate that Fe<sup>3+</sup> ions were uniformly dispersed in 1 (Figure S13 in the SI); (4) the fast and simple regeneration method showed that interaction between 1 and Fe<sup>3+</sup> ions should be weak. Therefore, we speculate that Fe<sup>3+</sup> may be diffused into the channels of 1 or attached to the surface of 1 rapidly and the encapsulated Fe<sup>3+</sup> ions are responsible for the quenching of the luminescence.<sup>22</sup>

In summary, a unique 3D Tb-BTB framework containing two types of 1D channels was synthesized with high yield and high thermostability. Compound 1 detects Fe<sup>3+</sup> ions with relatively high selectivity and sensitivity among 15 kinds of metal ions. Most importantly, 1 represents the recyclable luminescent probe for Fe<sup>3+</sup> ions, in which 1 can be simply and quickly recycled many times.

## ■ ASSOCIATED CONTENT

### ● Supporting Information

X-ray crystallographic data in CIF format (CCDC-1029691), synthesis, IR, TGA, PXRD, XPS, and luminescent spectra. The Supporting Information is available free of charge on the ACS Publications website at DOI: 10.1021/acs.inorgchem.5b00113.

## ■ AUTHOR INFORMATION

### Corresponding Author

\*E-mail: zhaobin@nankai.edu.cn. Fax: (+86)-22-23502458.

### Notes

The authors declare no competing financial interest.

## ■ ACKNOWLEDGMENTS

This work was supported by the 973 Program (Grants 2012CB821702 and 2011CB935902), NSFC (Grants 21421001 and 21473121), 111 Project (Grant B12015), and MOE Innovation Team (Grants IRT13022 and IRT-13R30) of China.

## ■ REFERENCES

- (1) Luo, J. H.; Xu, H. W.; Liu, Y.; Zhao, Y. S.; Daemen, L. L.; Brown, C.; Timofeeva, T. V.; Ma, S. Q.; Zhou, H. C. *J. Am. Chem. Soc.* **2008**, *130*, 9626–9627.
- (2) Chen, B. L.; Wang, L. B.; Zapata, F.; Qian, G. D.; Lobkovsky, E. B. *J. Am. Chem. Soc.* **2008**, *130*, 6718–6719.
- (3) Liu, W. S.; Jiao, T. Q.; Li, Y. Z.; Liu, Q. Z.; Tan, M. Y.; Wang, H.; Wang, L. F. *J. Am. Chem. Soc.* **2004**, *126*, 2280–2281.
- (4) Dang, S.; Ma, E.; Sun, Z. M.; Zhang, H. J. *J. Mater. Chem.* **2012**, *22*, 16920–16926.
- (5) Wu, M. Y.; Jiang, F. L.; Yuan, D. Q.; Pang, J. D.; Qian, J. J.; Al-Thabaiti, S. A.; Hong, M. C. *Chem. Commun.* **2014**, *50*, 1113–1115.

- (6) Li, Y. Y.; Yan, B.; Li, Q. P. *Dalton Trans.* **2013**, *42*, 1678–1686.
- (7) Liu, G. F.; Qiao, Z. P.; Wang, H. Z.; Chen, X. M.; Yang, G. *New J. Chem.* **2002**, *26*, 791–795.
- (8) (a) Zhao, X. Q.; Cui, P.; Zhao, B.; Shi, W.; Cheng, P. *Dalton Trans.* **2011**, *40*, 805. (b) Hou, Y. L.; Cheng, R. R.; Xiong, G.; Cui, J. Z.; Zhao, B. *Dalton Trans.* **2014**, *43*, 1814–1820.
- (9) (a) Hu, Z. C.; Deibert, B. J. D.; Li, J. *Chem. Soc. Rev.* **2014**, *43*, 5815–5840. (b) Chen, B. L.; Xiang, S. C.; Qian, G. D. *Acc. Chem. Res.* **2010**, *43*, 1115–1124. (c) Evans, O. R.; Lin, W. B. *Acc. Chem. Res.* **2002**, *35*, 511–522. (d) Guo, H. L. Y.; Zhu, Z.; Qiu, S. L.; Lercher, J. A.; Zhang, H. J. *Adv. Mater.* **2010**, *22*, 4190–4192.
- (10) (a) Zhao, B.; Chen, X. Y.; Cheng, P.; Liao, D. Z.; Yan, S. P.; Jiang, Z. H. *J. Am. Chem. Soc.* **2004**, *126*, 15394–15395. (b) Zhao, B.; Chen, X. Y.; Chen, Z.; Shi, W.; Cheng, P.; Yan, S. P.; Liao, D. Z. *Chem. Commun.* **2009**, 3113. (c) Zhao, B.; Gao, H. L.; Chen, X. Y.; Cheng, P.; Shi, W.; Liao, D. Z.; Yan, S. P.; Jiang, Z. H. *Chem.—Eur. J.* **2006**, *12*, 149. (d) Shi, P. F.; Zhao, B.; Xiong, G.; Hou, Y. L.; Cheng, P. *Chem. Commun.* **2012**, *48*, 8231. (e) Shi, P. F.; Hu, H. C.; Zhang, Z. Y.; Xiong, G.; Zhao, B. *Chem. Commun.* **2015**, *51*, 3985. (f) Hou, Y. L.; Xu, H.; Cheng, R. R.; Zhao, B. *Chem. Commun.* **2015**, *51*, 6769–6772.
- (11) Yang, C. X.; Ren, H. B.; Yan, X. P. *Anal. Chem.* **2013**, *85*, 7441–7446.
- (12) Hou, G. G.; Liu, Y.; Liu, Q. K.; Ma, J. P.; Dong, Y. B. *Chem. Commun.* **2011**, *47*, 10731–10733.
- (13) Tang, Q.; Liu, S. X.; Liu, Y. W.; Miao, J.; Li, S. J.; Zhang, L.; Shi, Z.; Zheng, Z. P. *Inorg. Chem.* **2013**, *52*, 2799–2801.
- (14) Zheng, M.; Tan, H. Q.; Xie, Z. G.; Zhang, L. G.; Jing, X. B.; Sun, Z. C. *ACS Appl. Mater. Interfaces* **2013**, *5*, 1078–1083.
- (15) (a) Chen, B. L.; Eddaoudi, M.; Hyde, S. T.; O’Keeffe, M.; Yaghi, O. M. *Science* **2001**, *291*, 1021–1023. (b) Chae, H. K.; Siberio-Perez, D. Y.; Kim, J.; Go, Y.; Eddaoudi, M.; Matzger, A. J.; O’Keeffe, M.; Yaghi, O. M. *Nature* **2004**, *427*, 523–527. (c) Gedrich, K.; Senkowska, I.; Klein, N.; Stoeck, U.; Henschel, A.; Lohe, M. R.; Baburin, I. A.; Mueller, U.; Kaskel, S. *Angew. Chem., Int. Ed.* **2010**, *49*, 8489–8492.
- (16) (a) Li, J.; Huang, P.; Wu, X. R.; Tao, J.; Huang, R. B.; Zheng, L. S. *Chem. Sci.* **2013**, *4*, 3232. (b) Wang, R. M.; Wang, Z. Y.; Xu, Y. W.; Dai, F. N.; Zhang, L. L.; Sun, D. F. *Inorg. Chem.* **2014**, *53*, 7086.
- (17) (a) Devic, T.; Serre, C.; Audebrand, N.; Marrot, J.; Férey, G. *J. Am. Chem. Soc.* **2005**, *127*, 12788–12789. (b) Lin, Z. J.; Zou, R. Q.; Xia, W.; Chen, L. J.; Wang, X. D.; Liao, F. H.; Wang, Y. X.; Lin, J. H.; Burrell, A. K. *J. Mater. Chem.* **2012**, *22*, 21076–21084.
- (18) Li, Q. W.; Liu, J. L.; Jia, J. H.; Leng, J. D.; Lin, W. Q.; Chen, Y. C.; Tong, M. L. *Dalton Trans.* **2013**, *42*, 11262–11270.
- (19) (a) Li, H.; Eddaoudi, M.; O’Keeffe, M.; Yaghi, O. M. *Nature* **1999**, *402*, 276–279. (b) Yang, S. H.; Lin, X.; Lewis, W.; Suyetin, M.; Bichoutskaia, E.; Parker, J. E.; Tang, C. C.; Allan, D. R.; Rizkallah, P. J.; Hubberstey, P.; Champness, N. R.; Thomas, K. M.; Blake, A. J.; Schröder, M. *Nat. Mater.* **2012**, *11*, 710–716. (c) Zheng, S. T.; Zhao, X. S.; Fuhr, L. A.; Feng, P. Y.; Bu, X. H. *J. Am. Chem. Soc.* **2013**, *135*, 10270–10273.
- (20) Cheng, Q. J.; Dong, Y. W.; Kang, M.; Zhang, P. *J. Lumin.* **2014**, *156*, 91–96.
- (21) Jiang, C. Q.; Wang, T. *Bioorg. Med. Chem.* **2004**, *12*, 2043–2047.
- (22) Kessler, M. A. *Anal. Chem.* **1999**, *71*, 1540–1543.